Published in final edited form as:
*J Morphol*. 2010 May ; 271(5): 580–595. doi:10.1002/jmor.10818.

# Post-hatching development of *Alligator mississippiensis* ovary and testis

**Brandon C. Moore**[*], **Heather J. Hamlin**, **Nicole L. Botteri**, **Ashley N. Lawler**, **Ketan K. Mathavan**, and **Louis J. Guillette Jr.**
Department of Biology, 220 Bartram Hall, PO Box 118525, University of Florida, Gainesville, Florida, 32611-8525 USA

## Abstract

We investigated ovary and testis development of *Alligator mississippiensis* during the first five months post-hatch. To better describe follicle assembly and seminiferous cord development, we employed histochemical techniques to detect carbohydrate-rich extracellular matrix components in one-week, one-month, three-month, and five-month-old gonads. We found profound morphological changes in both ovary and testis. During this time, oogenesis progressed up to diplotene arrest and meiotic germ cells increasingly interacted with follicular cells. Concomitant with follicles becoming invested with full complements of granulosa cells, a periodic acid Schiff's (PAS)-positive basement membrane formed. As follicles enlarged and thecal layers were observed, basement membranes and thecal compartments gained periodic acid-methionine silver (PAMS)-reactive fibers. The ovarian medulla increased first PAS- and then PAMS-reactivity as it fragmented into wide lacunae lined with low cuboidal to squamous epithelia. During this same period, testicular germ cells found along the tubule margins were observed progressing from spermatogonia to round spermatids located within the center of tubules. Accompanying this meiotic development, interstitial Leydig cell clusters become more visible and testicular capsules thickened. During the observed testis development, the thickening tunica albuginea and widening interstitial tissues showed increasing PAS- and PAMS-reactivity. We observed putative inter-sex structures in both ovary and testis. On the coelomic aspect of testes were cell clusters with germ cell morphology and at the posterior end of ovaries, we observed "medullary rests" resembling immature testis cords. We hypothesize laboratory conditions accelerated gonad maturation due to optimum conditions, including nutrients and temperature. Laboratory alligators grew more rapidly and with increased body conditions compared to previous measured, field-caught animals. Additionally, we predict the morphological maturation observed in these gonads is concomitant with increased endocrine activities.

### Keywords

*Alligator mississippiensis*; ovary; testis; development; follicle assembly

A fundamental component of gonadal differentiation and development is the formation of a sex-specific extracellular matrix (ECM). Alligator gonads show diverging, sex-specific structural protein formation during embryonic development (Smith and Joss, 1995). At the end of the period of temperature-dependent sex determination (TSD), embryonic ovaries have an expanded cortex of germ and somatic cells lacking laminin-immunoreactivity, overlying a medulla of fragmenting, laminin-immunoreactive (IR) primary sex cords.

[*]Address correspondence to: Brandon C. Moore – Tulane University, Telephone: 504-862-8454, Fax: 504-988-6428, bmoore2@tulane.edu.

Within the ovarian medulla, epithelial cells rest on laminin-IR basement membranes lining expanding lacunae. Conversely, alligator gonads that develop a testicular morphology show a regressed cortex and a medulla of seminiferous cords invested with germ cells and defined by laminin-IR basement membranes. Both ovary and testis juxtapose a mesonephric kidney with laminin-IR glomeruli and renal tubules. Here, we expand on these pre-hatching observations through an investigation of the post-hatching development of the alligator gonad. We employ histochemical techniques to investigate further ontogenetic changes in ECM distribution and structure and relate these findings to morphological changes of the gonad, including germ cell maturation.

Ovarian follicle assembly occurs with the assembly of its basement membrane. This definitive ECM feature separates the oocyte and granulosa from the surrounding stromal and/or thecal elements of an ovarian follicle. Basement membranes are primarily composed of collagen interwoven with laminin (Rodgers and Rodgers, 2002). Additional components such as fibronectin, other proteoglycans, and polysaccarides augment this complex structure. Previously, we have demonstrated that follicle assembly is a post-hatching event in the American alligator (Moore et al., 2008). Initial stages of alligator oocyte maturation do not display either a complete, encircling complement of follicular (pre-granulosa) cells or evidence of a basement membrane separating the germ cell from stromal tissues. Oocytes surrounded by a complete complement of follicular cells and enclosed within a basement membrane were not observed until three months after hatching under laboratory rearing conditions (Moore et al., 2008).

Both mammalian granulosa and thecal cells express mRNA for basement membrane components, including collagen and laminin (Zhao and Luck, 1995). However, it is hypothesized that granulosa cells produce the majority of basement membrane components (Rodgers et al., 2003). Therefore, initiation of follicular basement membrane synthesis around alligator oocytes should be associated the organization of follicular cells. While morphological changes associated with follicle assembly have been characterized in the American alligator (Moore et al., 2008; Uribe and Guillette, 2000), here we expand the scope of our observations from three to five months post-hatching and examine the ontogeny of follicular basement membrane assembly in association with post-hatching ovary development.

A limited body of research has addressed alligator testis morphology during the post-hatching period (Forbes, 1940; Guillette et al., 1994; Smith and Joss, 1995). Hatchling alligator testes present seminiferous cords invested with Sertoli and germ cells. Flattened stroma cells separate cords and differentiated Leydig cells are not observed. Sertoli cells contain ovoid nuclei placed adjacent to the basement membrane and project a large volume of apical cytoplasm into the cord interior. Using a series of manuscripts from previous laboratory-based experiments, we can describe a rough developmental sequence. Seminiferous cords of four-month-old testes present “activity and growth, as evidenced by crowding of the cords, numerous mitotic figures, and some anastomosis of the cords” (Forbes, 1937). Six- and 12-month-old tubules contain only spermatogonia (Forbes, 1940) whereas spermatocytes were observed in 15- and 18-months-old testes, but spermatogenesis was not noted (Forbes, 1938; 1940). Thickening of the tunica albuginea, increased number of spermatogonia, and development of the seminiferous cord basement membrane occurred during this period. Husbandry practices and body morphometrics were mostly unreported in these studies; therefore, body conditions are unknown at given ages.

Here, we focus on the first five months of testicular development and contrast changes in ECM, especially in seminiferous cords and the testicular capsule, to those observed in the ovary. The lamina propria, the vascularized layer of connective tissues in contact with

Sertoli cells and spermatogonia, delimits seminiferous tubules. It is composed of two layers; an inner acellular basement membrane composed of primarily laminin and collagen fibrils (adding tensile strength) and an outer multicellular layer containing peritubular myoid and lymphatic cells (Siu and Cheng, 2004a; b). Basic similarities have been demonstrated between sauropsid and mammalian lamina propria, including the types and arrangements of both cells and cellular and extracellular fibers (Unsicker and Burnstock, 1975). Mammalian peritubular myoid and Sertoli cells cooperate in the production of lamina propria ECM (Maekawa et al., 1996; Weber et al., 2002). Collagen- and laminin immunoreactivity of seminiferous cord lamina propria increases over the first 10 post-natal days in rats (Gelly et al., 1989). Similarly, alligator lamina propria development has been observed to continue during post-natal morphological differentiation (Forbes, 1940). A focus of this research will characterize alligator lamina propria in terms of the basement membrane development and myoid cell morphology during the post-hatching period.

The ECM has traditionally been described to act as a physical barrier compartmentalizing tissues, supplying rigid or elastic mechanical tissue support, filtering fluids passing through the matrix, or passively regulating osmotic forces. However, ECM also establishes “microenvironments” which directly modulate cell behaviors, including growth, maturation, and differentiation (Rodgers and Rodgers, 2002) and enhanced survival and proliferation of granulosa cells *in vitro* (Huet et al., 2001). Similarly, collagen itself has been demonstrated to be a biologically active molecule in testis (Siu and Cheng, 2004a). The ECM is now recognized as an active regulator of endocrine signaling and steroidogenesis (Berkholtz et al., 2006b) and can act as a barrier against growth factors or bind growth factors and serve as a reservoir (Rodgers and Rodgers, 2002; Wang et al., 2008). The ovarian follicle basement membrane of the chicken stores biologically active molecules such as growth factors and binding proteins and maintains normal granulosa cell morphology during *in vitro* culture (Asem et al., 2000a). Changes in transcription factor expression involved in sex differentiation have been associated with changes in structural protein expression, including laminin and collagen, in pre- and post-natal rat gonads (Pelliniemi and Frojdman, 2001). Increased levels of steroidogenic enzyme expression in both theca and granulosa cells have been shown to be associated with, and possibly directly modulated by, changes in ovarian ECM (Huet et al., 1997; Huet et al., 2001). In contrast, type IV collagen down regulates gonadotropin induced steroidogenesis in Leydig cells (Diaz et al., 2005). Isolated basement membrane components increased progesterone production in granulosa cells isolated from chicken ovarian follicles (Asem et al., 2000b). Therefore, this investigation of ECM distribution and development in hatchling alligator gonads not only elaborates structural maturation of these gonads, but likely also predicts concomitant physiological, biochemical, or endocrine changes.

## MATERIALS AND METHODS

American alligator (*Alligator mississippiensis*, Daudin, 1801) eggs were obtained from nests in the Lake Woodruff National Wildlife Refuge (Permit #WX01310) in June, 2006. American alligator sex determination is temperature dependent (Ferguson and Joanen, 1983). Eggs were obtained prior to the period of sex determination, returned to the University of Florida, and candled for viability. Eggs (n = 105) from seven clutches were divided between two incubation temperatures: 30°C that produces females (n = 55) and 33°C that produces males (n = 50). Within each incubation temperature group, eggs were systematically arranged in trays of damp moss and trays were rotated throughout incubation to minimize possible clutch biases. The total hatching success rate was 84%: 82% of animals from 30°C (n = 45) and 86% of animals from 33°C (n = 43).

All animal procedures conformed to an IACUC approved protocol. Following hatching, animals were housed in tanks within a temperature-controlled animal room (~20 neonates/ 0.7 $m^3$), experienced a 16:8 photoperiod with heat lamps for basking, and ambient room temperatures ranged from 27°C to 31°C. Alligators hatch with a relatively large residual yolk mass; thus hatchlings were fed *ad lib* starting 10 days after hatching with a small pellet size, commercial alligator chow (Burris Mills, LA).

Subsets of animals were killed using a lethal dose of sodium pentobarbital at: one week (30°C n = 12, 33°C n = 10), one month (30°C n = 11, 33°C n = 9), three months (30°C n = 10, 33°C n = 8), and five months post hatching (30°C n = 11, 33°C n = 10). Gonads and underlying mesonephric and adrenal tissues were removed as a single sample and fixed in Bouin's fixative for 24 hours. After fixation, tissues were washed in distilled water, dehydrated in a series of graded alcohols, cleared, paraffin embedded, and serially sectioned parasagittally at 6 μm. Tissue sections were stained with Masson's trichrome (Humason, 1979), periodic acid-Schiff (PAS)-Alcian blue (pH 2.5) with hematoxylin counterstain, or Gomori's periodic acid-methionine silver (PAMS) with an omission of gold toning and nuclear fast red counterstain. Tissues were examined with an Olympus BH-2 light microscope and photographed with a Pixelink PL-B623CU 3.0 megapixel digital camera.

Periodic acid-Schiff stains periodate reactive molecules containing a high proportion of carbohydrate and glycoconjugate macromolecules (glycogen, glycoproteins, and proteoglycans), typically found in connective tissues, mucus, and basement membranes. Laminin is a PAS-positive glycoprotein component of basement membranes that attaches non-connective tissue cells to collagenous fibers. Periodic acid-methionine silver staining detects argyrophilic molecules including collagenous reticular fibers (thin structural elements that provide supporting framework to many organs) and components of basement membranes. This technique has a broad specificity (Puchtler and Waldrop, 1978) and therefore direct inference of specific PAMS staining targets, especially in alligator, cannot be made at this time. However, silver staining techniques have successfully been used to stain glomerular mesangial matrix and Bowman's capsule of mammals (Adler et al., 2000; Harvey et al., 1998) and alligators (Moore and Hyndman, 200X), both collagen-rich structures (Abrass et al., 1988).

Microscopic examination of gonads showed all animals incubated at 30°C had ovaries whereas 68% of animals incubated at 33°C had testes. Of the females produced from the 33°C incubation, 92% came from three of the seven egg clutches collected for the experiment. Only results from gonads of 30°C females and 33°C males are presented in this manuscript. Snout-vent lengths (SVL) and body masses (BM) were recorded prior to dissections (average age of each group in days at measurement: one week = 4.5 d, one month = 28.1 d, three months = 88.5 d, and five months = 145.6 d) and body measurements were statistically compared by dissection ages and sex using two-way ANOVA and Newman-Keuls post-hoc analysis (JMP 7, SAS Institute). Samples sizes are presented in Fig. 1B. To assess possible growth trajectory differences due to experimental conditions, we compared these laboratory-raised animals to data taken from a cohort of field-captured, Lake Woodruff juvenile animals (field-captured cohort: female $n = 40$, male $n = 49$).

Examining the ovarian histology, morphological and histochemical changes in both cortex and medulla were observed. States of oogenesis and folliculogenesis, along with the presence and distribution of PAS- and PAMS-positive ovarian material, were characterized at each dissection time point. Chromatin and cytoplasmic morphologies were used to determine various stages of prophase I of oogenesis. Additionally, oocyte stages were identified according to a system that incorporates both meiotic characteristic and extent of folliculogenesis (Uribe and Guillette, 2000). Stage-1 oocytes exhibit meiotic germ cells at a

pre-diplotene stage often with fibrillar chromatin and in loose association with follicular cells. Stage-2 oocytes display an incomplete follicular layer of somatic cells and diplotene nuclei that often display chiasma, lampbrush chromosomes, and several nucleoli. Stage-3 oocytes, also diplotene, are distinctly larger in diameter than Stage-2 oocytes, often displaying lampbrush chromosomes, and possess a complete follicular layer of granulosa as well as a developing layer of surrounding thecal cells.

Testicular histology, including morphological and histochemical changes in the seminiferous cords, interstitial spaces, and the testicular capsule was observed. Ranges of testicular capsule thicknesses were estimated using optical micrometer measurements. Germ cell maturation was characterized by cellular morphology and location within tubules, with insight from the recent characterization of adult alligator germ cell maturation (Gribbins et al., 2006).

## RESULTS

### Somatic Growth, Gonad Placement, and Surrounding Tissues

During the first five months after hatching, alligators displayed robust growth in body mass and length (Fig. 1A–C). Average body masses for both males and females more than quadrupled between months one and three and then doubled between months three and five. Female BM and SVL were greater than male at months one and three, no differences were observed at one week or five months. Laboratory conditions increased BM growth in relation to SVL over measurements from field-captured animals (Fig. 1C).

Hatchling alligator gonads are thin, laminar tissues located on the caudal, dorsal peritoneal cavity wall. During post-hatch development, the anterior-medial aspect of the gonad is found lateral to the adrenal gland, whereas the medial- posterior aspect of the gonad is ventral to the degenerating mesonephric kidneys and large lymphatic vessels. Morphologically, the adrenal glands present intermingled aggregates of highly basophilic chromaffin cells and less basophilic intrarenal cells with each cell type clearly demarcated by PAS-positive (Figs. 2A, 7B) and PAMS-positive (not shown) extracellular matrix. The mesonephros contains renal corpuscles and associated ducts. Glomeruli show strong PAS (Fig. 6A) and PAMS reactivity (Fig. 6C). In one-week-old animals, the separation between gonad and adrenal gland or mesonephros is thin and irregular. Ovarian medullary tissues are not clearly demarcated from underlying mesonephric tissues. Testicular tubules are often separated from kidney structures by thin segments of connective tissue (Fig. 6A). During the first five months post-hatching, the connective tissues between gonad and adrenal gland (Fig. 7B) or mesonephrose thicken and separation between the organs becomes more pronounced.

### Ovary

At 10 days after hatching, the ovarian cortex is composed of a series of interconnected germ cell nests (Fig. 2A,C) containing oogonia clusters and Stage-1 (S1) oocytes. S1 oocytes present meiotic chromosomes and begin to show physical interactions with adjacent somatic cells (Fig. 2A). Nests are separated by trabecula, peninsula-like extensions of the medullary connective tissue into the cortex layer. Some trabeculae, when sectioned at oblique angles, appear in cross-section as islands of PAS/PAMS reactive tissues within germ cell nests (Fig. 2A,C).

Unlike the cortex, the ovarian medulla presents a fine meshwork matrix of PAS-and PAMS-positive materials. These materials encircle lacuna (Fig. 2A) and define the basement membranes on which cuboidal to low cuboidal epithelial cells of the lacunae rest. Lacunae spaces contain PAS and PAMS reactive secretory materials. On the edges of the lacuna

spaces, round voids in this secretory material were observed. The cortex/medulla boundary is clearly defined by the limit of medullary PAS- and PAMS-positive materials (Fig. 2A,C). The medullary region directly underlying the cortex, including the trabeculae, display greater PAMS reactivity compared to the remainder of medullary tissues (Fig. 2C).

One month after hatching, the ovarian cortex has greater numbers of oocytes with meiotic chromatin, but only S1 oocytes (Fig. 2B,D). The cortex continues to be separated from the medulla by a distinct boundary of PAS- and PAMS-reactive materials. Periodic acid-methionine silver reactivity throughout the medulla, especially at the cortex/medulla boundary, is more robust than at one week after hatching (Fig. 2D). Sporadic somatic cells on the coelomic epithelium of the cortex show PAS reactivity. In the medulla, lacuna diameter increased while interstitial tissues decreased (Fig. 2B). Concomitant with the change in lacunae diameter, lacunae epithelial cells are more often squamous to low cuboidal than cuboidal in shape. Secretory materials in the expanded lacunae continue to be both PAS- and PAMS-positive.

At three months after hatching, the ovarian cortex is thickened and is populated with oogonia and S1 to Stage-3 (S3) oocytes (Figs. 3A,C and 4A–C). Germ cell nests present single and multinucleated oocytes with condensed, meiotic chromatin and juxtanuclear Balbiani bodies in their ooplasms (Fig. 4A,C). Stage-2 (S2) oocytes have large spherical nuclei containing lampbrush chromosomes (Fig. 4B), PAS-positive Balbiani bodies (Fig. 5B), and are incompletely surrounded by follicular cells. Follicle assembly around S2 oocytes is associated with a thin PAS-positive basement membrane (Fig. 5B), although it does not always fully surround the follicle. The basement membrane forming around S2 oocytes is not PAMS-positive (Fig. 3D and 4B). An increased number of squamous somatic cells on the coelomic epithelium of the cortex show PAS reactivity (Fig. 3A) compared to one month after hatching (Fig. 2A).

Complete follicular layers enclose S3 oocytes. A monolayer of granulosa cells is bounded by PAS/PAMS-positive basement membranes and oocyte cytoplasms have prominent PAS/PAMS-positive Balbiani bodies (Figs. 3A,C and 4C). Fibrous thecal layers are first observed surrounding S3 follicles. Periodic acid-Schiff/periodic acid-methionine silver positive fibers intertwine thecal layers and segregate the follicles from the remainder of the germinal nests of the cortex. S3 oocytes are always found in contact with some aspect of the cortex/medulla interface and the PAS/PAMS-positive fibrous materials of the basement membranes are often contiguous with morphologically similar medullary fibers (Figs. 2A,C and 4C). Most epithelial cells of the lacunae are low cuboidal to squamous in shape and often directly juxtapose epithelial cells of adjacent lacunae due to the lack of interstitial tissues (Figs. 2A,C and 4B,C).

At five months after hatching, proliferation of S2 and S3 oocytes contributes to the continued thickening of the cortex (Figs. 3B,D and 5A,B). Oocyte expansion results in convolution of germ cell nests in the cortex. Nests wrap around the enlarging follicles, disrupting their previous, relatively uniform arrangements. Periodic acid-Schiff positive materials around somatic cells located at the coelomic epithelium are more prevalent (Figs. 3B and 5A,B). Multi-oocytic follicles, two or more oocytes in a follicle encompassed by a single basement membrane, are infrequently observed (Fig. 5A). The morphology of medulla at five month after hatching is similar to that observed at three months.

In the most posterior aspect of some ovaries of various ages are small, distinct regions of tissue, previously termed the “medullary rest” (Forbes, 1937). If present, this medullary rest is posterior to the termination of the cortex and adjacent to the posterior end of the medulla. The medullary rest lies under a thick tunica albuginea and contains poorly formed tubules,

defined by PAS-positive basement membranes (Fig. 5C). The interior of these tubules contain cells with germ cell-like morphologies. Squamous cells intercalate within the tubule basement membranes. Around the tubules, interstitial tissues contain cells with Leydig-like morphologies.

### Testis

One week after hatching, single layers of Sertoli cells and spermatogonia resting on a basement membrane line seminiferous cords (Fig. 6A). Sertoli cytoplasmic projections fill the cords and lumens are not observed. Cords are demarcated by fine PAS- and PAMS-positive basement membranes (Fig. 6A,C) that are internal to simple squamous layers of peritubular myoid cells. Interstitial tissues are sparse. Leydig cells are not observed and interstitial cells present irregularly shaped nuclei. Alligator testes are not divided into lobules by way of fibrous septa. Within a thin (~5 μm) testicular capsule seminiferous cords branch and anastomose freely. A tunica serosa of squamous cells lies over a fibrous, PAS-positive tunica albuginea (Fig. 6A); however the testicular capsule is not PAMS reactive at this age (Fig. 6C).

One month after hatch, the testicular capsule is thicker (5–10 μm) than at one week after hatching and is both PAS- and PAMS-positive (Fig. 6B,D, respectively). In the tunica albuginea, squamous cells are interspersed with fibers running parallel to the coelomic epithelium. The volume of interstitial tissue is greater than at one week and small clusters of cells now exhibit Leydig-like morphology with round nuclei and larger cytoplasms. A more robust PAMS-positive layer bounds seminiferous cords (Fig. 6D). Within the cords, spermatogonia, with large round nuclei, are sporadically found lying off the basement membrane (Fig. 6B). These putative spermatogonia type B did not display meiotic chromatin.

At three months after hatching, testes exhibit distinct morphological changes. Seminiferous cords observed at one month after hatching are now seminiferous tubules containing germ cells in a variety of meiotic states (Fig. 7A). Toward the center of the tubules are primary spermatocytes with increased nuclear and cytoplasmic sizes and condensed chromatin. Thin PAS- and PAMS-positive basement membrane and surrounded by simple, squamous layers of peritubular myoid cells continue to define seminiferous tubules. However, these myoid cells show an increased frequency of overlapping cytoplasms giving them a pseudo-stratified appearance. The volume of interstitial tissues has further increased and presents clusters of Leydig cells with relatively large well-defined cytoplasm, surrounded by PAS- and PAMS-positive fibrous ECM. The testicular capsule continues to thicken (30–50 μm). Fenestrations in the tunica albuginea that join with seminiferous tubules are observed (Fig. 7A,C). At these fenestrations, the PAS- and PAMS-positive basement membranes of the seminiferous tubules merge with fibrous components of the testicular capsule.

Morphological changes initially observed at three months after hatching continue at five months after hatching. The testicular capsule thickened (40–65 μm) and continued to exhibit infrequent fenestrations to the coelomic cavity. Interstitial tissue volumes expand and present large clusters of Leydig cells, often found within a matrix of PAS and PAMS-positive fibers (Figs. 7B,D and Figs. 8A–C). Seminiferous tubules contain developing germ cells including primary spermatocytes and round spermatids (Figs. 7B,D and 8A–C). Round spermatids present dense nuclei without visible chromosome fibers. Apical Sertoli cell cytoplasmic projections do not fully fill some tubules containing early, round spermatids, suggesting the formation of a luminal compartment in these tubules (Figs. 7B,D and 8A–C). Infrequently, clusters of round cells lay on the coelomic side of the tunica albuginea. These cells do not resemble squamous cells of the tunica serosa and putatively are germ cells that are a remnant of incomplete cortex regression during gonadal differentiation (Fig. 8C).

## DISCUSSION

During the first five months after hatching, we observed profound morphological changes in alligator gonads. In ovaries, germ cells entered into meiotic progressions, follicular cells organized around oocytes, steroidogenic cells organized around follicles, and medullary regions transformed into a matrix of expanded lacunae. In testes, we observed meiotic germ cells, clusters of steroidogenic cells became apparent, interstitial tissues expanded, and both seminiferous tubules and the testicular capsules matured. Intercalated within these gonadal architectural changes were pronounced developments in the ECM that we visualized using histochemical stains. Periodic acid Schiff reactivity clearly delineated the ovarian cortex and medulla, marked the formation of follicular basement membranes, defined the lamina propria of seminiferous tubules, and showed the thickening of the testicular capsule. Periodic acid methionine silver reactivity marked the maturation of follicles in both their basement membrane and Balbiani bodies and also testicular composition of the lamina propria, interstitial space, and capsule. In light of these observations, we propose that the gonadal ECM is playing a role beyond that of acting only as a structural framework for the organ.

Follicle assembly and early maturation observed in this study agrees with previous observations in which one-month-old alligator ovaries exhibit only S1 oocytes, whereas three-months-old ovaries had S1 to S3 oocytes (Moore et al., 2008). Here, we have demonstrated that in five-month-old ovaries, the frequency of S2 and S3 oocytes increases compared to three months. Additionally, we have observed the formation and modification of ovarian ECM during this developmental period.

Ovarian follicular ECM is a spatially and temporally dynamic structure that remodels in accordance to the developmental state of the follicle (Berkholtz et al., 2006a; Irving-Rodgers and Rodgers, 2006; Mazatid et al., 2005). A distinct temporal pattern of laminin and collagen formation around mouse follicles has been observed (Berkholtz et al., 2006a). During folliculogenesis, between the vascularized theca and the avascular granulosa a basement membrane is deposited. The basement membranes of primordial follicles, composed of laminin, encompass the exterior of the granulosa. Later, follicles acquire type I collagen during the transition to primary follicles and type IV collagen and fibronectin as the granulosa expands in secondary follicles. Type IV collagen is also found predominantly in thecal layers and, to a lesser extent, in granulosa and stroma. As follicular maturation commences, type IV collagen increases around the theca and thickens between granulosa and stroma.

Postnatal follicle assembly is similar in pigs and rabbits. In one-day-old pig ovaries, germ cell nests are encircled by laminin-positive basement membranes and contain mitotic oogonia and meiotic oogonia (Lee et al., 1996). Follicle assembly in these nests commences where they juxtapose the medulla, forming primordial follicles that exhibit laminin-positive basement membranes. Similar to the pig, five-day-old rabbit ovaries display germ cell nests circumscribed by a laminin-positive matrix, whereas collagen fibers are not detectable (Lee et al., 1996). At 14 days post-natal, basement membranes encircle rabbit primary follicles. In post-natal ovaries of both pig and rabbit, laminin-positive materials are observed spanning from the ovarian surface epithelium to the ovarian rete and define the apical and basal aspects of germ cell nests. Additionally, collagen is not observed until the initiation of follicle maturation.

The changes in ovarian ECM associated with alligator follicle assembly are in agreement with these observations. From one week to one month after hatching, germ cell nests are bounded by a PAS-positive ECM along the cortex/medulla boundary and at the cortex/

coelomic boundary by distinct aggregates. This localization of PAS-reactivity is similar to laminin-IR observed previously at hatching (Smith and Joss, 1995). Three months after hatch, PAS-positive material at the cortex/coelomic boundary is more pronounced and the cortex/medulla boundary becomes increasingly convoluted with the initiation of follicle assembly. S2 oocytes begin to exhibit PAS-positive basement membranes concomitant with increasing interaction with follicular cells. S3 oocytes enclosed in follicles with complete complements of follicular cells and a theca layer present a PAS- and PAMS-positive follicular ECM layer, indicative of the presence of both laminin and type IV collagen.

The formation of a thecal layer concomitant with the detection of PAMS-positive materials suggests an interaction of collagenous ECM development and an alteration in the follicles steroidogenic capacity. S3 oocytes are always observed with some direct contact to the cortex/medulla boundary. In chicken ovaries, granulosa cells of small follicles are steroidogenically inactive (Nitta et al., 1993) and steroidogenic cells recruit to theca layers from the medulla (Narbaitz and Derobert, 1968; Pedernera et al., 1988; Sekido and Lovell-Badge, 2007). The direct connections of PAMS-positive fibers of the medulla and those of the theca layers of S3 oocytes supports the hypothesis that the recruitment of steroidogenic cells into the alligator cortex layer is similar to that observed in chickens (Moore et al., 2008). A small percentage of follicles contained more than one S3 oocyte. These multioocytic follicles (MOFs) did not present similar PAS- or PAMS-positive material between the multiple oocytes as was observed between the oocytes and follicular cells. A similar morphology has been observed in six-month-old ovaries in which S3 oocytes and a few multi-oocytic follicles “extend more deeply into the medulla” (Forbes, 1940).

Additionally, PAS-positive Balbiani bodies (asymmetrical aggregates of RNA and organelles including endoplasmic reticulum, Golgi, and mitochondria) that are observed in S1 through S3 oocytes gain PAMS reactivity in S3 oocytes. Balbiani bodies of birds are reactive to silver stains (Guraya, 1962); however, how this shift in reactivity relates to development or maturation of Balbiani bodies is unknown.

The ovarian medulla undergoes substantial remodeling during the post-hatching period. At 10 days after hatching, the ovarian medulla is primarily PAS-positive and shows signs of fragmentation. Periodic acid methionine silver reactivity is observed primarily in the basement membrane underlying epithelial cells of the lacunae. The lacunae, PAS- and PAMS-positive secretory materials presented peripheral spherical voids that we propose result from lipid deposits removed during histological clearing. In hatchling chickens, steroidogenic cells derived from the primary sex cords reside in the medulla (Gonzalezmoran et al., 1985; Narbaitz and Derobert, 1968). If these steroidogenic cells are also present in the alligator medulla, putative lipid droplets could supply substrates for steroidogenesis. Further histological examination is needed to ascertain if these structures are derived from lipid aggregates.

During this post-hatching period, PAMS reactivity in the medulla increases as lacunae expand and interstitial tissues diminish. At one year of age, the alligator medulla consists of numerous thin strands of laminin-IR connective tissue which form the walls of lacunae (Ferguson and Joanen, 1983; Smith and Joss, 1995). The progression of morphological developments observed in this study over the first five months post-hatching is in agreement with the observed morphology in one-year-old alligator medulla. We hypothesize that the alligator ovarian medulla is a responsive, endocrine tissue and is capable of influencing ovarian development (Edwards et al., 2006; Moore et al., 2008). Therefore, these morphological changes most likely influence the physiology of the entire ovary.

At the posterior aspect of ovaries throughout the growth period, we observed small adjunct tissues previously referred to as a 'medullary rest'. These tissues have been previously observed in ovaries of 18- and 21-month-old alligators and were noted to resemble testis of 6-month-old alligator (Ferguson and Joanen, 1983; Forbes, 1937; 1938) and our current observations support these previous studies.

During the first five months after hatching, profound changes occurred in testicular morphology. From a 10-day-old testis containing spermatogenic cords invested with spermatagonia resting against the basal lamina, we observed subsequent maturation resulting in spermatogenic tubules containing meiotic and post-meiotic germ cells in the tubule interiors and putative lumen formation. This germ cell maturation was concomitant with increased interstitial tissues, the establishment of prominent Leydig cell clusters, and increased PAS and PAMS reactivity of the tunica and interstitial regions. We observed the greatest maturation during the prodigious body mass doubling observed between three and five months post-hatching. Therefore, to put these morphological observations in context, an examination of interactions between alligator body size or condition, sexual maturation, and seasonality is necessary.

The minimum size for sexual maturity in male alligators has been reported as ~100 cm SVL (Joanen and McNease, 1980). In wild-caught adult alligators, initiation of spermatogenesis was observed in mid-February (Gribbins et al., 2006; Lance, 1989) and sperm has been found in the penile sulcus of wild-caught alligators from May to June (Joanen and McNease, 1980). Spermiation ceased in late June at the conclusion of the breeding season and was followed by testicular regression (Gribbins et al., 2006; Joanen and McNease, 1980). However, alligators held in controlled environments have shown deviations from seasonal reproductive and growth cycles. Sperm has been observed in the penile sulcus of animals kept in a heated enclosure in mid-winter (Cardeilhac, 1981). Alligator growth can be limited by resource availability, habitat suitability, population density, growing season length, and salinity (Saalfeld et al., 2008), but temperature is a primary factor modulating growth (Lance, 2003). Alligator growth is more rapid in heated, controlled environments than in the wild (Coulson and Hernandez, 1983; Herbert et al., 2002; Joanen and McNease, 1989). If animals are raised in heated enclosures (~31°C) with ambient photoperiod, alligator growth can be decoupled from seasonal patterns and exhibit steady increasing body mass and length during the first year of growth (Herbert et al., 2002). Conversely, low temperatures or poor nutrition can impede sexual maturity (Lance, 2003).

Our group has demonstrated seasonal elevations of circulating testosterone concentrations in wild male alligator that have attained a SVL > 38 cm (Rooney et al., 2004). In wild juvenile Florida alligators, a strong correlation has been observed between SVL and BM (Guillette et al., 2000) and also SVL and age (Milnes et al., 2002). These studies were performed using animals from a defined geographic range of Florida that share similar environmental conditions. In contrast, animals in this study experienced rearing conditions that were quite different from those experienced by wild animals: stable elevated temperature, lack of environmental variability, lack of predator pressures, and constant access to food. This resulted in alteration of the growth trajectory with our captive-raised animals, attaining greater body masses per unit SVL than field-caught animals. Furthermore, field-caught alligators with a SVL of 38 cm have body masses (~1100 g) that are similar to those of five-month-old, laboratory-raised alligators with SVLs of ~32 cm. We propose that an initiation of sexual maturation marked by increases in circulating testosterone concentrations observed in field animals > 38 cm could be more related to an attainment of a threshold body mass or condition index than of a specific length, in light of the testis maturation observed in five-month-old laboratory animals with similar body masses, but shorter SVLs.

In light of this prodigious body growth and putative precocious gonadal maturation, we observed a testicular maturational pattern more similar to domestic chickens than wild alligators. In hatchling chicken testes, seminiferous tubules do not exhibit lumens and are surrounded by compact interstitial tissues of undifferentiated mesenchyme and few Leydig cells (Gonzalez-Moran, 1997). Spermatogonia proliferate concomitantly with an increase in tubule diameter at 5 weeks of age; spermatocytes are observed at week six (Kumaran and Turner, 1949). With the initiation of meiosis, spermatids are observed between weeks 8–12 post-hatch (Bergmann and Schindelmeiser, 1987; Kumaran and Turner, 1949). Leydig cell growth accompanies tubule expansion. This morphological progression in chicken testis over three months has temporal and morphological similarities to our observations in alligator testes over the five months post-hatching and is clearly in conflict with a maturational timeline of wild, male alligators. But it should also be noted, that the traditional description of testicular maturation/sexual maturation at 1 m SVL in wild animals is also unlikely as wild juvenile males of 38 cm snout vent length or greater exhibit seasonal variation in plasma testosterone concentration and their testes are likely to be similar in development to that described in the present study.

A comparison of the morphological development observed in these laboratory-raised alligator testes to other vertebrates can provide a more refined characterization of the level of maturation in these animals. Comparing the morphological development observed in these laboratory-raised alligator testes to other vertebrates, we can better characterize the level of maturation observed in these animals. In many vertebrates, male germ cell development begins in the basal epithelial compartment of the seminiferous tubule, where they are sheathed in the cytoplasmic folds of Sertoli cells (Siu and Cheng, 2004b). As development continues, germ cells migrate inward, toward the medial aspect of the tubule, and eventually exit the blood-testis barrier (BTB) formed by tight junctions between Sertoli cells and enter the apical/adluminal compartment. The BTB is an immunological barrier segregating post-meiotic germs cells from the systemic antibodies of the host organism. Germ cells developed up to preleptotene spermatocyte stage (diploid) are found within the BTB whereas pachytene spermatocytes (haploid) and later developmental stages are found outside of the BTB. A BTB is formed either before puberty (mouse, man), during pubescent initiation of meiosis in others (dog, rabbit), or after the onset of meiosis (sauropsids) (Bergmann et al., 1984; Siu and Cheng, 2004b). In chicken testis, BTB formation occurs around eight weeks of age, after the initiation of meiosis, and concomitant with early spermatid (haploid germ cell) formation (Bergmann and Schindelmeiser, 1987). Chicken tubules containing these early spermatids and BTB do not possess lumens. We observed round spermatids (haploid) and evidence of lumen formation in the testes of five-month-old laboratory-raised alligators. If alligator testis maturation is similar to chicken, then these animals should have produced a BTB.

Recent characterization of alligator spermatogenesis (Gribbins et al., 2006) has allowed new insight into post-hatching alligator testicular development. A previous investigation of six-month-old alligator testes by our group showed seminiferous tubules containing both spermatogonia and meiotic germ cells and interstitial spaces containing Leydig cell clusters (Guillette et al., 1994). Within this study, animals hatched from eggs collected from Lake Woodruff, a national wildlife reserve, and raised with supplemental heat displayed testes containing germ cells developed up to round spermatid stage. The testes of five-month-old, Lake Woodruff animals described in this manuscript share many of the morphologies observed in the six-month-old animals from the previous study, including Leydig cell development and evidence of spermatogenesis. In contrast, six-month-old testes from animals hatched from eggs collected from Lake Apopka, a highly-contaminated environment (Guillette et al., 1999), showed germ cells in seminiferous tubule centers that displayed “bar-shape nuclei”. In light of the morphological maturation during alligator

spermatogenesis (Gribbins et al., 2006), these cells are probably later-stage spermatids initiating nuclei elongation. Before dissection, these animals underwent an ovine luteinizing hormone (LH) challenge with daily injections for two days. This treatment significantly increased circulating estradiol-17β ($E_2$) levels in Lake Apopka animals (~3.3 times greater), but did not alter Lake Woodruff animal $E_2$ levels. Recent research has demonstrated that both LH and $E_2$ modulate the transition of round spermatids to elongating spermatids. Additionally, treatment with the aromatizable androgen testosterone propionate has induced the formation of elongated spermatids in juvenile crocodile testes (Ramaswam and Jacob, 1965).

In LHβ-subunit knockout mice, spermatogenesis is halted at the round spermatid stage (Ma et al., 2004). LH has been demonstrated to regulate aromatase expression in rat Leydig cells (Genissel et al., 2001) and epididymis (Shayu and Rao, 2006), while Sertoli and germ cells may also produce estrogens (Carreau et al., 2006). Mice with disrupted aromatase expression are infertile due to failure to elongate round spermatids (Robertson et al., 1999). Taken together, an LH challenge resulting in increased circulating $E_2$ levels provides a hypothesis explaining the production of elongating spermatids in six-month-old alligator testes. Why this response was observed in Lake Apopka animals, but not in Lake Woodruff animals is unknown, however, research has demonstrated altered gonadotropin signaling and testis morphology resulting from herbicide exposure (Shariati et al., 2008).

During the five-month post-hatching period, we observed thickening of an originally thin and discontinuous testicular capsule. The alligator tunica is similar to testicular capsules of birds being composed of a thin tunica serosa, an outermost layer formed from the peritoneum, overlying the tunica albuginea composed of a thick layer of smooth muscle-like cells, fibroblasts, collagen bundles, and elastic fibers (Aire and Ozegbe, 2007). We observed both PAS- and PAMS-positive staining of the tunica albuginea, but not the tunica serosa. The capsule encompassed the entire testis and did not divide the sex cords into lobules. In contrast, testes of pituitary extract treated 21-month-old alligators displayed a thickened tunica and septa dividing testis lobules, though septa were not observed in control animals (Forbes, 1937). Our observations are in agreement with a lack of septa in juvenile alligator testes, similar to the morphology of bird testes (Aire and Ozegbe, 2007).

In association with tunica development, we observed two intriguing and possibly associated morphologies. Clusters of cells resembling germinal epithelium were infrequently found on the coelomic aspect of the tunica. Putative germ cells on the peritoneal side of the tunica albuginea have been previously observed in post-hatching alligator testes (Forbes, 1937; 1940). Furthermore, these clusters were more frequently observed at six months than at three months, initiating a hypothesis that these cortical cells could proliferate during this time period (Forbes, 1940). In this study, these clusters were more often observed in older animals in which we noted the initiation of spermatogenesis and also openings in the tunica where the medullary cords directly interfaced with the peritoneum. These fenestrations connected medullary tubules containing meiotic germ cells to the external aspect of the tunica, a morphology previously observed in 6, 15, 18, and 21-month-old alligators (Forbes, 1937; 1938; 1940). Furthermore, clusters of germ cells have been previously observed passing through these openings in the tunica albuginea and forming “isolated cortical proliferations”. With *in vivo* estrone treatment these cortical projections proliferated and expanded over the peritoneal tunica (Forbes, 1938), therefore, demonstrating these cells show endocrine responsivity. Research describing primitive sex cord formation in turtles showed cord formation resulted from an invagination of the coelomic epithelium with the basal lamina of sex cords being continuous with basal lamina of the coelomic epithelium (Yao et al., 2004). We propose the fenestration observed in alligator testes may be

developmentally related to the invaginations observed in turtle testes, with the coelomic epithelium giving rise to somatic cells of the sex cords.

From our current and previous observations, hypotheses regarding these cortical cells can be formulated. First, these cortical cells may be remnants of the regressing cortex during sex differentiation that becomes more prominent during later post-hatching development. Second, these cortical cells are derived from the medulla through either an incomplete tunica during early testicular development or from medullary tubules opening through pronounced fenestration in the tunica. Lastly, cortical cells could be derived through a combination of both mechanisms. Regardless of the mechanism, the presence of germ cells on the testis coelomic epithelia and the medullary rest morphology observed in ovaries shows that post-hatching alligator gonads display distinctive morphologies that deviate from archetypical testis and ovary.

## Acknowledgments

We greatly thank Rex A. Hess and Mari Carmen Uribe-Aranzabal for their assistance and advice in assessing and interpreting histological images. This study was made possible by the continuing logistical support of our alligator research by the Florida Fish and Wildlife Conservation Commission; specifically we thank Allan Woodward for his continued assistance with fieldwork and permitting. This work was supported in part by grants to LJG from the NIH (R21 HD047885-01; R21 ES014053-01) and the Howard Hughes Medical Institute Professors program.

## LITERATURE CITED

Abrass CK, Peterson CV, Raugi GJ. Phenotypic-Expression Of Collagen Types In Mesangial Matrix Of Diabetic And Nondiabetic Rats. Diabetes. 1988; 37(12):1695–1702. [PubMed: 3056764]

Adler SG, Feld S, Striker L, Striker G, LaPage J, Esposito C, Aboulhosn J, Barba L, Cha DR, Nast CC. Glomerular type IV collagen in patients with diabetic nephropathy with and without additional glomerular disease. Kidney Int. 2000; 57(5):2084–2092. [PubMed: 10792628]

Aire TA, Ozegbe PC. The testicular capsule and peritubular tissue of birds: morphometry, histology, ultrastructure and immunohistochemistry. J Anat. 2007; 210(6):731–740. [PubMed: 17451470]

Asem EK, Feng SL, Stingley-Salazar SR, Turek JJ, Peter AT, Robinson JP. Basal lamina of avian ovarian follicle: influence on morphology of granulosa cells in-vitro. Comp Biochem Physiol C. 2000a; 125(2):189–201.

Asem EK, Stingley-Salazar SR, Robinson JP, Turek JJ. Effect of basal lamina on progesterone production by chicken granulosa cells in vitro - influence of follicular development. Comp Biochem Physiol C. 2000b; 125(2):233–244.

Bergmann M, Schindelmeiser J. Development Of The Blood-Testis Barrier In The Domestic-Fowl (*Gallus domesticus*). Int J Androl. 1987; 10(2):481–488. [PubMed: 3610358]

Bergmann M, Schindelmeiser J, Greven H. The Blood-Testis Barrier In Vertebrates Having Different Testicular Organization. Cell Tissue Res. 1984; 238(1):145–150.

Berkholtz CB, Lai BE, Woodruff TK, Shea LD. Distribution of extracellular matrix proteins type I collagen, type IV collagen, fibronectin, and laminin in mouse folliculogenesis. Histochem Cell Biol. 2006a; 126(5):583–592. [PubMed: 16758163]

Berkholtz CB, Shea LD, Woodruff TK. Extracellular matrix functions in follicle maturation. Seminars In Reproductive Medicine. 2006b; 24(4):262–269. [PubMed: 16944423]

Cardeilhac, PT. Reproductive physiology of the American alligator. Proceeding of the 1st Annual Alligator Production Conference; Gainesville: University of Florida; 1981.

Carreau S, Delalande C, Silandre D, Bourguiba S, Lambard S. Aromatase and estrogen receptors in male reproduction. Mol Cell Endocrinol. 2006; 246(1–2):65–68. [PubMed: 16406261]

Coulson, RA.; Hernandez, T. Alligator Metabolism: Studies On Chemical-Reactions In vivo. Elmsford, New York: Pergamon Press Inc; 1983. Natural History; p. 1-14.

Diaz ES, Pellizzari E, Casanova M, Cigorraga SB, Denduchis B. Type IV collagen induces down-regulation of steroidogenic response to gonadotropins in adult rat Leydig cells involving mitogen-activated protein kinase. Mol Reprod Dev. 2005; 72(2):208–215. [PubMed: 16037942]

Edwards TM, Moore BC, Guillette LJ. Reproductive dysgenesis in wildlife: a comparative view. Int J Androl. 2006; 29(1):109–120. [PubMed: 16466531]

Ferguson MWJ, Joanen T. Temperature-Dependent Sex Determination In *Alligator mississippiensis*. J Zool. 1983 JUN.200:143–177.

Forbes TR. Studies on the reproductive system of the alligator I. The effects of prolonged injections of pituitary whole gland extract in the immature alligator. Anat Rec. 1937; 70(1):113–137.

Forbes TR. Studies on the reproductive system of the alligator II The effecfs of prolonged injections of oestrone in the immature alligator. J Exp Zool. 1938; 78(3):335–367.

Forbes TR. Studies of the Reproductive System of the Alligator IV. Observations of the Development of the Gonad, the Adrenal Cortex, and the Mullerian Duct. Contrib Embryol. 1940; 174:131–154.

Gelly JL, Richoux JP, Leheup BP, Grignon G. Immunolocalization Of Type-IV Collagen And Laminin During Rat Gonadal Morphogenesis And Postnatal-Development Of The Testis And Epididymis. Histochemistry. 1989; 93(1):31–37. [PubMed: 2613546]

Genissel C, Levallet J, Carreau S. Regulation of cytochrome P450 aromatase gene expression in adult rat Leydig cells: comparison with estradiol production. J Endocrinol. 2001; 168(1):95–105. [PubMed: 11139774]

Gonzalez-Moran G. A stereological study of the different cell populations in chicken testes treated with follicle-stimulating hormone during embryonic development. Anat Histol Embryol. 1997; 26(4):311–317. [PubMed: 9400050]

Gonzalezmoran G, Gonzalezdelpliego M, Pedernera E. Morphological-Changes In The Ovary Of Newly Hatched Chickens Treated With Chorionic-Gonadotropin During Embryonic-Development. General And Comparative Endocrinology. 1985; 59(1):162–167. [PubMed: 4018552]

Gribbins KM, Elsey RM, Gist DH. Cytological evaluation of the germ cell development strategy within the testis of the American alligator, *Alligator mississippiensis*. Acta Zoologica. 2006; 87(1): 59–69.

Guillette LJ, Brock JW, Rooney AA, Woodward AR. Serum concentrations of various environmental contaminants and their relationship to sex steroid concentrations and phallus size in juvenile American alligators. Arch Environ Contam Toxicol. 1999; 36(4):447–455. [PubMed: 10227864]

Guillette LJ, Crain DA, Gunderson MP, Kools SAE, Milnes MR, Orlando EF, Rooney AA, Woodward AR. Alligators and endocrine disrupting contaminants: A current perspective. Am Zool. 2000; 40(3):438–452.

Guillette LJ, Gross TS, Masson GR, Matter JM, Percival HF, Woodward AR. Developmental Abnormalities Of The Gonad And Abnormal Sex-Hormone Concentrations In Juvenile Alligators From Contaminated And Control Lakes In Florida. Environ Health Perspect. 1994; 102(8):680–688. [PubMed: 7895709]

Guraya SS. Structure And Function Of So-Called Yolk-Nucleus In Oogenesis Of Birds. Q J Microsc Sci. 1962; 103(4):411.

Harvey SJ, Zheng KQ, Sado Y, Naito I, Ninomiya Y, Jacobs RM, Hudson BG, Thorner PS. Role of distinct type IV collagen networks in glomerular development and function. Kidney Int. 1998; 54(6):1857–1866. [PubMed: 9853250]

Herbert JD, Coulson TD, Coulson RA. Growth rates of Chinese and American alligators. Comp Biochem Physiol A. 2002; 131(4):909–916.

Huet C, Monget P, Pisselet C, Monniaux D. Changes in extracellular matrix components and steroidogenic enzymes during growth and atresia of antral ovarian follicles in the sheep. Biol Reprod. 1997; 56(4):1025–1034. [PubMed: 9096887]

Huet C, Pisselet C, Mandon-Pepin B, Monget P, Monniaux D. Extracellular matrix regulates ovine granulosa cell survival, proliferation and steroidogenesis: relationships between cell shape and function. J Endocrinol. 2001; 169(2):347–360. [PubMed: 11312151]

Humason, GL. Animal Tissue Techniques. San Francisco: W.H. Freeman; 1979.

Irving-Rodgers HF, Rodgers RJ. Extracellular matrix of the developing ovarian follicle. Semin Reprod Med. 2006; 24(4):195–203. [PubMed: 16944417]

Joanen, T.; McNease, L. Reproductive Biology of the American Alligator in Southwest Louisiana. In: Murphy, JB.; Collins, JT., editors. Reproductive biology and disease of captive reptiles. Lawrence; Kansas: 1980. p. 153-159.

Joanen T, McNease LL. Ecology And Physiology Of Nesting And Early Development Of The American Alligator. Am Zool. 1989; 29(3):987–998.

Kumaran JDS, Turner CW. The Normal Development Of The Testes In The White Plymouth Rock. Poult Sci. 1949; 28(4):511–520.

Lance VA. Reproductive-Cycle Of The American Alligator. Am Zool. 1989; 29(3):999–1018.

Lance VA. Alligator physiology and life history: the importance of temperature. Exp Gerontol. 2003; 38(7):801–805. [PubMed: 12855291]

Lee VH, Britt JH, Dunbar BS. Localization of laminin proteins during early follicular development in pig and rabbit ovaries. J Reprod Fertil. 1996; 108(1):115–122. [PubMed: 8958837]

Ma XP, Dong YL, Matzuk MM, Kumar TR. Targeted disruption of luteinizing hormone beta-subunit leads to hypogonadism, defects in gonadal steroidogenesis, and infertility. Proc Natl Acad Sci U S A. 2004; 101(49):17294–17299. [PubMed: 15569941]

Maekawa M, Kamimura K, Nagano T. Peritubular myoid cells in the testis: Their structure and function. Arch Histol Cytol. 1996; 59(1):1–13. [PubMed: 8727359]

Mazatid S, Guyot R, Guig UJB, Coudoue N, Le Magueresse-Battistoni B, Margre S. Basal membrane remodeling during follicle histogenesis in the rat ovary: contribution of proteinase of the MMP and PA families. Dev Biol. 2005; 277(2):403–416. [PubMed: 15617683]

Milnes MR, Woodward AR, Rooney AA, Guillette LJ. Plasma steroid concentrations in relation to size and age in juvenile alligators from two Florida lakes. Comp Biochem Physiol A Comp Physiol. 2002; 131(4):923–930.

Moore BC, Hyndman KA. Morphology and Histochemistry of Juvenile American Alligator Nephrons. Anatomical Record. 2009; 292(10):1670–6.

Moore BC, Uribe-Aranzabal MC, Boggs ASP, Guillette LJ. Developmental morphology of the neonatal alligator (*Alligator mississippiensis*) ovary. J Morphol. 2008; 269(3):302–312. [PubMed: 17957708]

Narbaitz R, Derobert EM. Postnatal Evolution Of Steroidogenic Cells In Chick Ovary. Histochemie. 1968; 15(3):187. [PubMed: 4246253]

Nitta H, Mason JI, Bahr JM. Localization Of 3-Beta-Hydroxysteroid Dehydrogenase In The Chicken Ovarian Follicle Shifts From The Theca Layer To Granulosa Layer With Follicular Maturation. Biology Of Reproduction. 1993; 48(1):110–116. [PubMed: 8418898]

Pedernera E, Gomez Y, Velazquez P, Juarezoropeza MA, Delpliego MG. Identification Of Steroidogenic Cell Subpopulations In The Ovary Of The Newly Hatched Chicken. Gen Comp Endocrinol. 1988; 71(1):153–162. [PubMed: 3410293]

Pelliniemi LJ, Frojdman K. Structural and regulatory macromolecules in sex differentiation of gonads. J Exp Zool. 2001; 290(5):523–528. [PubMed: 11555860]

Puchtler H, Waldrop FS. Silver Impregnation Methods For Reticulum Fibers And Reticulin - Reinvestigation Of Their Origins And Specifity. Histochemistry. 1978; 57(3):177–187. [PubMed: 711512]

Ramaswam LS, Jacob D. Effect Of Testosterone Propionate On Urogenital Organs Of Immature Crocodile *Crocodylus palustris* Lesson. Experientia. 1965; 21(4):206. [PubMed: 5845262]

Robertson KM, O'Donnell L, Jones MEE, Meachem SJ, Boon WC, Fisher CR, Graves KH, McLachlan RI, Simpson ER. Impairment of spermatogenesis in mice lacking a functional aromatase (*cyp 19*) gene. Proc Natl Acad Sci U S A. 1999; 96(14):7986–7991. [PubMed: 10393934]

Rodgers RJ, Irving-Rodgers HF, Russell DL. Extracellular matrix of the developing ovarian follicle. Reproduction. 2003; 126(4):415–424. [PubMed: 14525524]

Rodgers RJ, Rodgers HFI. Extracellular matrix of the bovine ovarian membrana granulosa. Mol Cell Endocrinol. 2002; 191(1):57–64. [PubMed: 12044919]

Rooney AA, Crain DA, Woodward AR, Guillette LJ. Seasonal variation in plasma sex steroid concentrations in juvenile American alligators. Gen Comp Endocrinol. 2004; 135(1):25–34. [PubMed: 14644641]

Saalfeld DT, Webb KK, Conway WC, Calkins GE, Duguay JP. Growth and Condition of American Alligators (*Alligator mississippiensis*) in an Inland Wetland of East Texas. Southeast Nat. 2008; 7(3):541–550.

Sekido R, Lovell-Badge R. Mechanisms of gonadal morphogenesis are not conserved between chick and mouse. Dev Biol. 2007; 302(1):132–142. [PubMed: 17026980]

Shariati M, Noorafshan A, Mokhtari M, Askari HR. The Effects of Trifluralin on LH, FSH and Testosterone Hormone Levels and Testis Histological Changes in Adult Rats. Int J Fertil Steril. 2008; 2(1):23–28.

Shayu D, Rao AJ. Expression of functional aromatase in the epididymis: Role of androgens and LH in modulation of expression and activity. Mol Cell Endocrinol. 2006; 249(1–2):40–50. [PubMed: 16569475]

Siu MKY, Cheng CY. Dynamic cross-talk between cells and the extracellular matrix in the testis. Bioessays. 2004a; 26(9):978–992. [PubMed: 15351968]

Siu MKY, Cheng CY. Extracellular matrix: Recent advances on its role in junction dynamics in the seminiferous epithelium during spermatogenesis. Biol Reprod. 2004b; 71(2):375–391. [PubMed: 15115723]

Smith CA, Joss JMP. Immunohistochemical Localization Of Laminin And Cytokeratin In Embryonic Alligator Gonads. Acta Zoologica. 1995; 76(3):249–256.

Unsicker K, Burnstock G. Myoid Cells In Peritubular Tissue (Lamina-Propria) Of Reptilian Testis. Cell And Tissue Research. 1975; 163(4):545–560. [PubMed: 1201592]

Uribe MCA, Guillette LJ. Oogenesis and ovarian histology of the American alligator Alligator mississippiensis. J Morphol. 2000; 245(3):225–240. [PubMed: 10972971]

Wang XM, Harris RE, Bayston LJ, Ashe HL. Type IV collagens regulate BMP signaling in *Drosophila*. Nature. 2008; 455(7209):72–U49. [PubMed: 18701888]

Weber MA, Groos S, Aumuller G, Konrad L. Post-natal development of the rat testis: steroid hormone receptor distribution and extracellular matrix deposition. Andrologia. 2002; 34(1):41–54. [PubMed: 11996181]

Yao HHC, DiNapoli L, Capel B. Cellular mechanisms of sex determination in the red-eared slider turtle, *Trachemys scripta*. Mech Dev. 2004; 121(11):1393–1401. [PubMed: 15454268]

Zhao Y, Luck MR. Gene-Expression And Protein Distribution Of Collagen, Fibronectin And Laminin In Bovine Follicles And Corpora-Lutea. J Reprod Fertil. 1995; 104(1):115–123. [PubMed: 7636792]

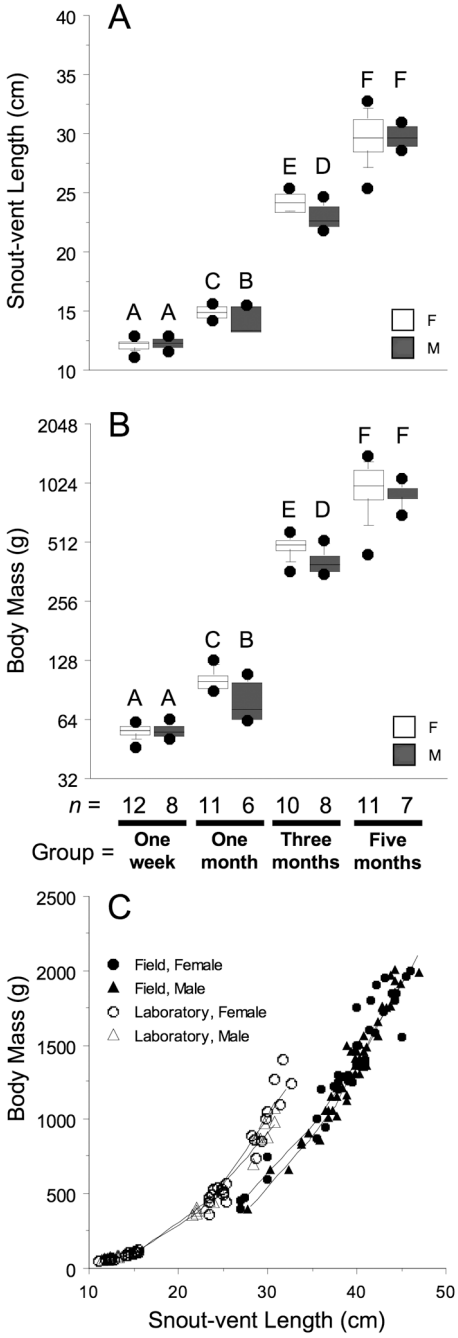


**Fig. 1.**

Box plot diagrams of **A**: snout-vent length and **B**: body mass (note log2 scale) for dissected animals grouped by age and sex (open boxes = female; grey boxes = male). Boxes define $75^{th}$ to $25^{th}$ percentiles and are bisected by the mean values. Whiskers define $90^{th}$ and $10^{th}$ percentiles with outliers (filled circles) above and below. Superscripts over boxes denote differences between groups ($P > 0.05$). Sample sizes for each group are set below graphs. **C**: A scatterplot diagram of snout-vent length and body mass for laboratory-raised animals (open figures) and field-captured, Lake Woodruff juvenile animals (solid figures). Males = triangles; females = circles. Individual locally weighted scatter plot smoother (LOWESS) curves (tension = 50) are plotted for each group.

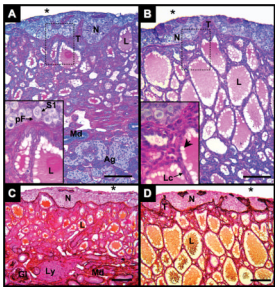


**Fig. 2.**

Ovary of *Alligator mississippiensis* in parasaggital view. **A**: One week after hatching stained with PAS/AB. **B**: One month after hatching stained with PAS/AB. **C**: One week after hatching stained with PAMS. **D**: One month after hatching stained with PAMS. Dotted line rectangles define areas shown in greater magnification in lower left of images. Scale bars = 100 *um*. Nest of germ cells (N); connective tissue trabeculae (T); coelomic cavity (*); stage-1 oocytes (S1); prefollicular cell (pF); lacunae (L); peripheral lacunae areas void of secretory materials (arrowhead); low cuboidal to squamous epithelial lacunae cells (Lc); adrenal tissue (Ag); glomeruli (Gl); mesonephric ducts (Md); and lymphatic aggregates (Ly).

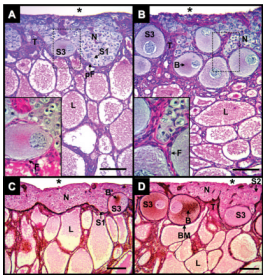


**Fig. 3.**

Ovary of *Alligator mississippiensis* in parasaggital view. **A**: Three months after hatching stained with PAS/AB. **B**: Five months after hatching stained with PAS/AB. **C**: Three weeks after hatching stained with PAMS. **D**: Five months after hatching stained with PAMS. Dotted line rectangles define areas shown in greater magnification in lower left of images. Scale bars = 100 *um*. Nest of germ cells (N); connective tissue trabeculae (T); coelomic cavity (*); stage-1, 2, and 3 oocytes (S1, S2, and S3, respectively); follicular cells (F); prefollicular cell (pF); lacunae (L); Balbiani bodies (B); and basement membrane (BM).

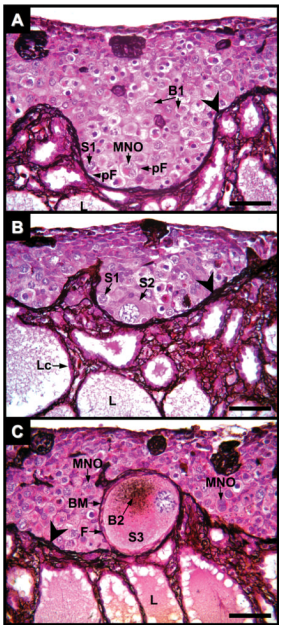


**Fig. 4.**

Ovary of *Alligator mississippiensis* at three months after hatching in parasaggital view stained with PAMS showing nests of germ cells in various stages of oocyte maturation. **A**: Cortical germ cell nests are delimited by PAMS-positive fibers (large arrowheads) which are contiguous fibers within the ovarian medulla. Stage-1 oocytes (S1) with early Balbiani bodies (B1) are in association with prefollicular cells (pF). Some S1 oocytes with diplotene chromatin are multi-nucleated (MNO). Medullary lacunae (L). **B** and **C**: Stage-2 (S2) and -3 (S3) oocytes are in cortical regions directly adjacent with the medulla. S2 oocytes display enlarged ooplasm, but lack a complete layer of cells and surrounding basement membrane. Stage-3 oocytes are completely encircled by follicular cells (F) and a PAMS-positive basement membrane (BM) and often display a PAMS-positive Balbiani body (B2). Lacunae epithelial cells (Lc) lay upon a basement membrane composed of PAMS-positive fibers. Scale bars = 100 *um*.

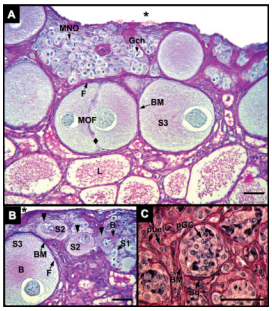


**Fig. 5.**

Ovary of *Alligator mississippiensis* at five months after hatching in parasaggital view stained with PAS/AB showing nests of germ cells in various stages of oocyte maturation and location. **A** and **B**: Cortical germ cells with mitotic chromosomes (Gch) and uni-nucleated (S1) and multinucleated (MNO) Stage-1 oocytes with diplotene chromatin are observed in germ cell nests. Stage-2 (S2) and -3 (S3) oocytes are observed in regions with direct connection to an adjacent medulla. S2 oocytes display enlarged ooplasms, PAS-positive Balbiani bodies (B), and a thin, irregular PAS-positive basement membrane (black triangles), but lack a distinct full complement of encircling follicular cells. S3 oocytes display PAS-positive Balbiani bodies (B). In contrast to S2 oocytes, S3 oocytes have a complete ring of follicular cells (F) and a distinct, encompassing PAS-positive basement membrane (BM). S3 oocytes may be contained in a multioocytic follicle (MOF) with a lack of follicular cells and basement membrane demarcation between germ cells (diamond). Coelom = (*). **C**: Putative germ cells (pGC) are observed in tubules within the medullary rest of the alligator ovary. A PAS-positive basement membrane (BM) associated with squamous, myoid-like cells (Sq) encompasses an aggregate of putative germ cells with large cytoplasms and displaying nuclei with fibrous chromatin. Interstitial tissues display cells with Leydig cell morphology (pLe). Scale bars = 50 *um*.

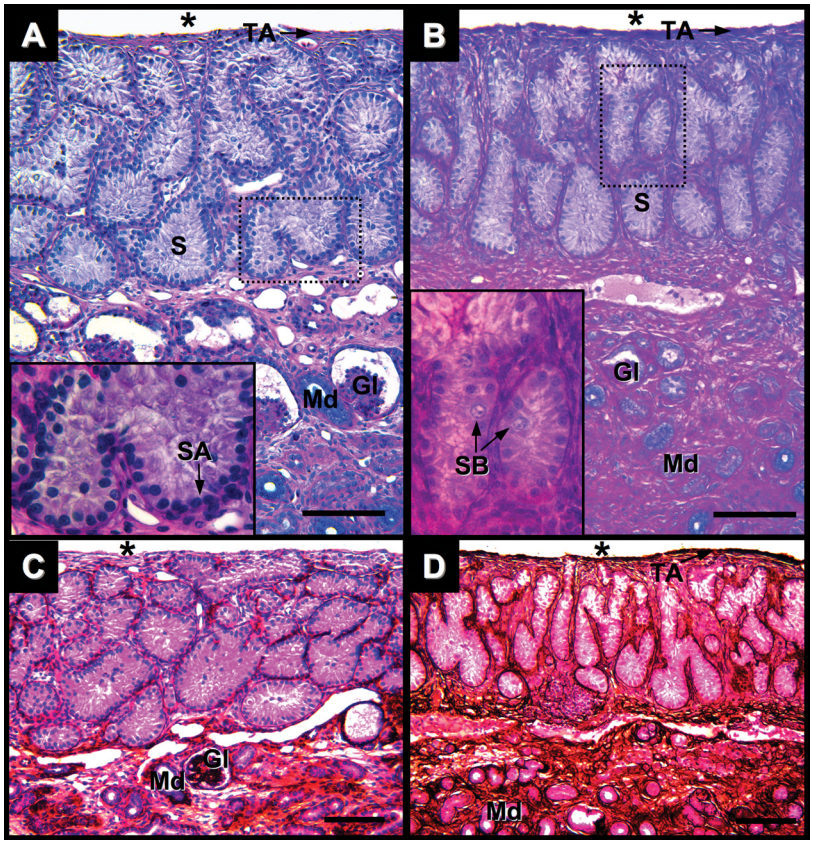


**Fig. 6.**

Testis of *Alligator mississippiensis* in parasaggital view. **A**: One week after hatching stained with PAS/AB. **B**: One month after hatching stained with PAS/AB. **C**: One week after hatching stained with PAMS. **D**: One month after hatching stained with PAMS. Dotted line rectangles define areas shown in greater magnification in lower left of images. Scale bars = 100 *um*. Coelomic cavity (*); tunica albuginea (TA); seminiferous cords (S); spermatogonia A and B (SA and SB, respectively); glomeruli (Gl); and mesonephric ducts (Md).

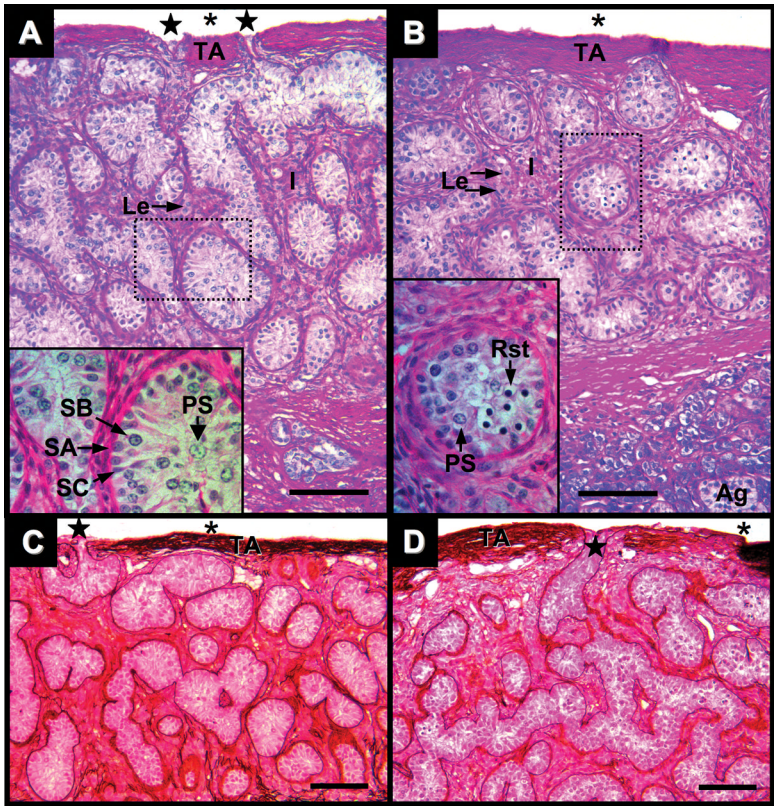


**Fig. 7.**

Testis of *Alligator mississippiensis* in parasaggital view. **A**: Three months after hatching stained with PAS/AB. **B**: Five months after hatching stained with PAS/AB. **C**: Three weeks after hatching stained with PAMS. **D**: Five months after hatching stained with PAMS. Dotted line rectangles define areas shown in greater magnification in lower left of images. Scale bars = 100 *um*. Tunica albuginea (TA); coelomic cavity (*); fenestration (star); interstitial tissues (I), Leydig cells (Le); Sertoli cells (SC); spermatogonia A and B (SA and SB, respectively); primary spermatocytes (PS), round spermatids (Rst), and adrenal tissue (Ag).

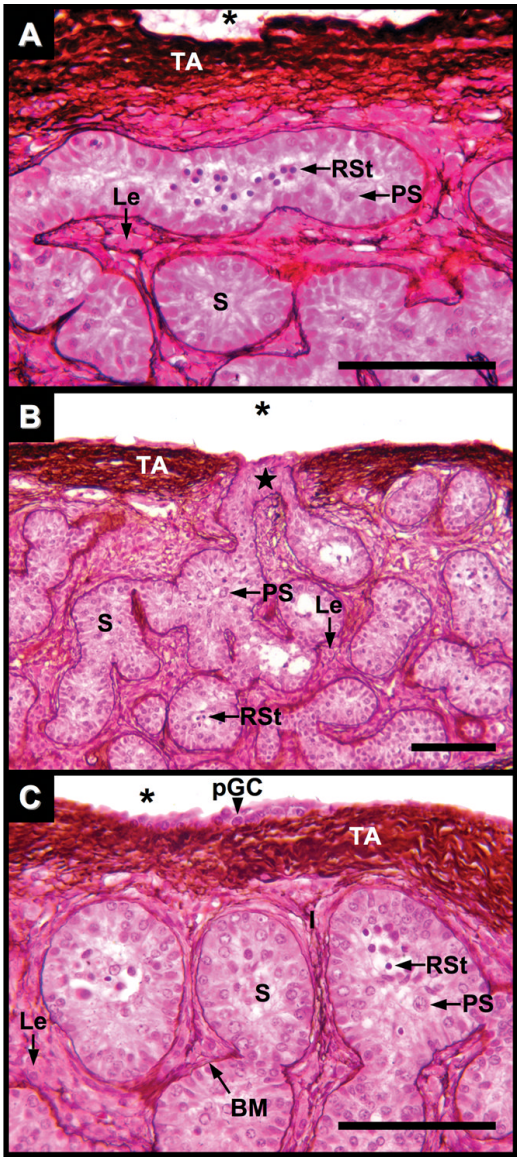


**Fig. 8.**

Testis of *Alligator mississippiensis* at five months after hatching in parasaggital view stained with PAMS. **A** and **B**: Seminiferous tubules (S) lie within a robust tunica albuginea (TA) of PAMS-positive fibers bordering the coelom (*). Occasional fenestrations connect seminiferous tubules to the coelomic cavity (star). Tubule basement membranes (BM) and surrounding interstitial tissues show PAMS-positive fibers. Primary spermatocytes (PS); Round spermatids (RSt). Clusters of Leydig cells (Le) are interspersed within the interstitial tissues. **C**: Putative germ cells are occasionally observed on the coelomic side of the tunica (pGC). Scale bars = 100 *um*.